CrossMark

Adsorption of poly(styrenesulfonate) onto different-sized alumina particles: characteristics and mechanisms

Tien Duc Pham[1] · Thi Uyen Do[1] · Thu Thao Pham[1] · Thi Anh Huong Nguyen[1] · Thi Kim Thuong Nguyen[1] ·
Ngoc Duy Vu[1] · Thanh Son Le[1] · Cuong Manh Vu[2,3] · Motoyoshi Kobayashi[4]

Abstract

We report the adsorption characteristics and mechanisms of a strong polyanion, poly(styrenesulfonate), PSS, onto α-Al$_2$O$_3$ with large size (L-Al$_2$O$_3$) and small size (S-Al$_2$O$_3$) in this paper. Some effective conditions to the adsorption of PSS onto L-Al$_2$O$_3$ and S-Al$_2$O$_3$ such as adsorption time, pH, mass ratio of PSS to α-Al$_2$O$_3$, and ionic strength were systematically studied. Maximum adsorption capacities of PSS onto both L-Al$_2$O$_3$ and S-Al$_2$O$_3$ were achieved with adsorption time 120 min, mass ratio of PSS to α-Al$_2$O$_3$ 20 mg/g, and ionic strength 50 mM NaCl. The PSS adsorption onto S-Al$_2$O$_3$ significantly decreased with increasing pH from 4 to 9 while PSS adsorption onto L-Al$_2$O$_3$ decreased insignificantly in the pH range 4–9. Adsorption of PSS onto both L-Al$_2$O$_3$ and S-Al$_2$O$_3$ increased with increasing salt from 0 to 50 mM NaCl, indicating that electrostatic and none-lectrostatic interactions controlled adsorption at low ionic strength. However, adsorption of PSS was independent on the ionic strength at salt concentration higher than 50 mM. The changes in surface charge after PSS adsorption onto L-Al$_2$O$_3$ and S-Al$_2$O$_3$ were determined by zeta potential while the differences of surface functional groups before and after PSS adsorption were characterized by Fourier-transform infrared spectroscopy (FT-IR). The zeta potential as a function of the mass ratio of PSS to L-Al$_2$O$_3$ and S-Al$_2$O$_3$ agreed well with the adsorption capacity against the mass ratio. Adsorption mechanisms of PSS onto L-Al$_2$O$_3$ and S-Al$_2$O$_3$ were also discussed based on the changes in zeta potential, the differences of surface functional groups, and adsorbed amount as a function of the mass ratio of PSS to α-Al$_2$O$_3$.

Keywords Polyelectrolyte adsorption · α-Alumina · PSS · Particle size

Introduction

Adsorption of polyelectrolyte (polyanion or polycation) on solid surface is an interesting research topic in

✉ Tien Duc Pham
tienduchphn@gmail.com; tienducpham@hus.edu.vn

✉ Thanh Son Le
sonlt@vnu.edu.vn

✉ Cuong Manh Vu
vumanhcuong309@gmail.com

1 Faculty of Chemistry, VNU – University of Science, Vietnam National University, Hanoi, 19 Le Thanh Tong, Hoan Kiem, Hanoi 10000, Vietnam

2 Center for Advanced Chemistry, Institute of Research and Development, Duy Tan University, Da Nang, Vietnam

3 Chemical Department, Le Quy Don Technical University, 236 Hoang Quoc Viet, Hanoi, Vietnam

4 Faculty of Life and Environmental Sciences, University of Tsukuba, Tennodai 1-1-1, Tsukuba, Ibaraki 305-8572, Japan

interface science and soft matter. The main applications of polyelectrolytes in water and wastewater treatment are coagulation and flocculation [1]. In most case of flocculation in the presence of polyelectrolytes, adsorption characteristics of polyelectrolytes on particle surfaces play an important role for evaluating flocculation behavior of particles. Nevertheless, adsorption of polyelectrolyte is complex due to the charge effect, especially for the case that solid surface also contains electrical charge. For the adsorption of strong polyelectrolyte on oppositely charged surface, driving force can only be electrostatic or a combination of electrostatic and non-electrostatic interactions [2, 3]. Due to specific adsorption characteristics and mechanisms of polyelectrolyte on the solid surface, many polyelectrolytes were used to modify solid particles to enhance removal efficiency of both organic and inorganic pollutants [4–7]. Therefore, numerous studies investigated adsorption of polyelectrolyte in many systems in which the adsorption of polyelectrolyte is complicated due to the charging behavior of adsorbents and polyelectrolytes [8–14]. Poly(styrenesulfonate) (PSS) is a strong anionic

polyelectrolyte, so that its structure is pH independent and it is a high-charge density polymer. PSS contains strong ultraviolet (UV) chromophores of benzenesulfonate group that can be directly monitored by UV absorption spectroscopy [15]. Adsorption of PSS on colloidal particles [16–18], large beads [19], thin film, or membrane [20, 21] was studied by many physicochemical methods such as UV spectroscopy, Fourier-transform infrared spectroscopy (FT-IR), fluorescence spectrophotometry, atomic force microscopy (AFM), and inductively couple plasma atomic emission spectrometry (ICP-AES).

Metal oxides are well-known adsorbents that are widely used for study of polyelectrolyte adsorption [10, 12, 22–24]. However, charging behavior of metal oxide strongly depends on pH due to the amphoteric nature property [25–27]. In some cases, charge regulation of metal oxide upon adsorption of electrolyte occurs so that the change in surface charge is complicated [19, 28]. Wolterink et al. [28] demonstrated that a significant effect of pH and the small effect of ionic strength on the adsorbed amount, while charge regulation still took place with PSS adsorption on hematite particle. On the other hand, Pham et al. [19] indicated that PSS adsorption onto large α-Al$_2$O$_3$ beads induced the proton concomitant at low ionic strength while PSS adsorption capacity increased with increasing ionic strength.

The degree of polymerization or molecular weight plays an important role for polyelectrolyte adsorption [2, 19, 29]. The PSS adsorption with different molecular weights onto colloidal α-Al$_2$O$_3$ particles and α-Al$_2$O$_3$ beads was found to be similar characteristics [2, 19]. In these cases, PSS adsorbed amount per surface area of adsorbent (adsorption density) increased with increasing molecular weight. Another important factor is the effect of particle size of adsorbent. The different size distribution effectively changed adsorption characteristics due to the differences in charged surface and specific surface area. The effect of particle size of adsorbents on the adsorption in many systems was systematically studied [30–32]. However, to our best knowledge, the PSS adsorption onto different-sized Al$_2$O$_3$ has not been reported. The further perspective and inspiration of this system is to predict the mechanisms of natural polyelectrolytes onto the soils that mainly contain metal oxides including Al$_2$O$_3$. So far, the modification of soil particles by polyelectrolytes can be used to enhance the removal efficiency of organic pollutants in the environmental remediation. The polyelectrolyte adsorption changes charging behavior of soil containing metal oxides and organic matter due to the presence of charged groups in polyelectrolyte molecules. Since organic pollutants in aqueous solution basically have a charge, the electrostatic interaction plays an important role to attract the pollutants onto polyelectrolyte-modified soil surface [5, 33]. As a result, the removal efficiencies of pollutants increase significantly after surface modification of soil with polyelectrolytes [34].

In this study, for the first time, we investigated the adsorption of PSS onto α-Al$_2$O$_3$ with different particle sizes, named as large size (L-Al$_2$O$_3$) and small size (S-Al$_2$O$_3$). The effects of adsorption time, pH, mass ratio of PSS to α-Al$_2$O$_3$, and ionic strength on PSS adsorption were examined. Adsorption mechanisms of PSS onto L-Al$_2$O$_3$ and S-Al$_2$O$_3$ were suggested on the basis of the change in functional surface groups by FT-IR, surface charge change by electrokinetic (ζ potential) measurements, and adsorbed amount as a function of the mass ratio of PSS to α-Al$_2$O$_3$.

Experimental

Materials

High-purity alpha alumina (99.99%, Sumitomo, Chuo-ku, Osaka, Japan) has a large size with diameter of about 1600 nm (AA 1.5) denoted as L-Al$_2$O$_3$, while and a small-sized alpha alumina denoted as S-Al$_2$O$_3$ with a diameter of about 300 nm is used in the present study. Specific surface areas of L-Al$_2$O$_3$ and S-Al$_2$O$_3$, which were examined by the Brunauer–Emmett–Teller (BET) method using a surface area analyzer (Micromeritics, Gemini VII 2390), were found to be 7.85 m^2/g and 1.20 m^2/g, respectively. Both L-Al$_2$O$_3$ and S-Al$_2$O$_3$ were treated before using for other experiments according to our previously published papers [19, 35]: the raw α-Al$_2$O$_3$ particles were washed several times with 0.2 M NaOH before rinsing with ultrapure water to neutral pH, then dried at 110 °C and reactivated at 600 °C for 2 h. The treated α-Al$_2$O$_3$ was cooled in a desiccator at room temperature and stored in a polyethylene container.

Powder of sodium poly(styrene sulfonate), PSS, with a molecular weights of 1000 kg/mol was purchased from Sigma-Aldrich Chemical Co, Inc., with a degree of polymerization of 4850. The chemical structure of PSS is indicated in Fig. 1. Ionic strength and pH were adjusted by the addition of NaCl, HCl, and NaOH (Merck, Germany). All solutions in this study were prepared with ultrapure water using an ultrapure water system (Labconco, USA) with resistivity 18.2 MΩ cm.

Adsorption study

All adsorption experiments were conducted in batches. Firstly, 1 mg/mL (1000 ppm) of PSS stock solution was prepared by dissolving a precisely 1.0000 g of PSS into 1 L ultrapure water. Then, the stock solution was diluted with appropriate times based on experimental requirements.

A known amount of adsorbent suspension was thoroughly mixed with 10 mL of 0.1 mg/mL PSS solution in 15-mL Falcon tubes at 25 ± 2 °C controlled by air-conditioned laboratory. For adsorption time from 5 to
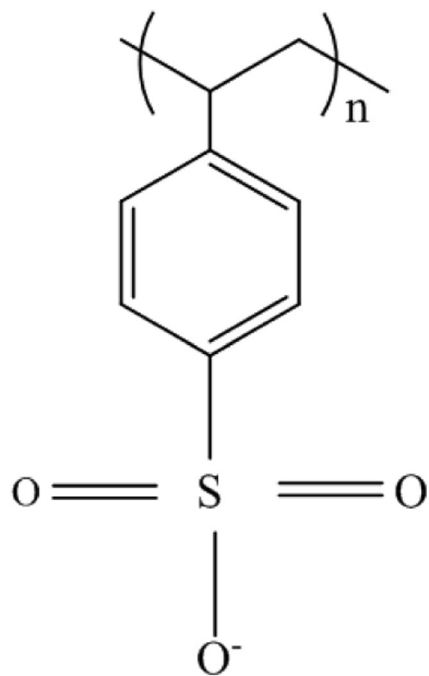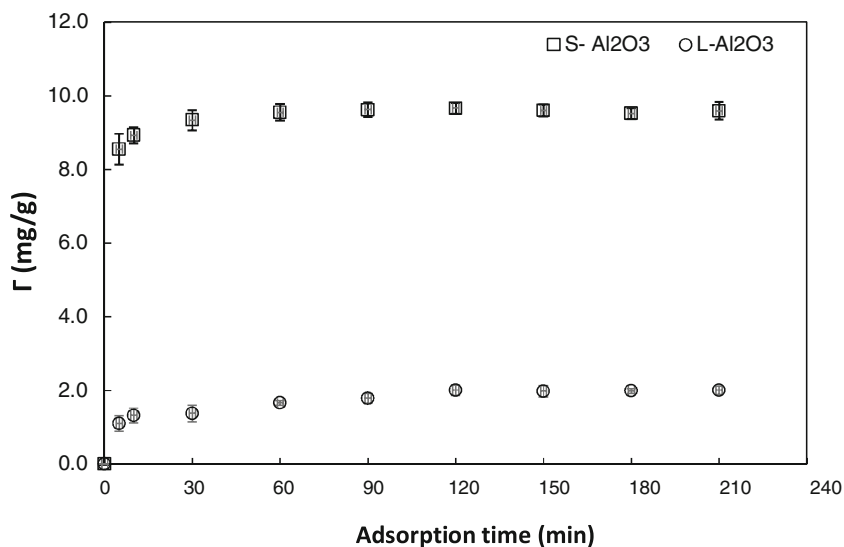
Fig. 1 The chemical structure of PSS

DIGISYSTEM—Taiwan). The effects of adsorptive conditions (pH, mass ratio of PSS to α-Al$_2$O$_3$, adsorption time, and ionic strength) were studied.

All concentrations of PSS in the supernatants were determined by spectrophotometric method at wavelength 261.8 nm with a quartz 10-mm path length cuvette using an UV-Vis spectrophotometer (UV-1650PC, Shimadzu). The UV-Vis method to quantify the PSS concentrations was indicated in our previously published paper [19]. The standard calibration curves of PSS in different ionic strength and pH have a correlation coefficient of at least 0.999. The PSS concentrations in the samples before and after adsorption were directly quantified by standard calibration curves. The adsorption capacity Γ (mg/g) of PSS onto α-Al$_2$O$_3$ was calculated by Eq. (1):

$$\Gamma = \frac{c_i - C_e}{m} \times 1000 \tag{1}$$

where C_i (mg/mL) and C_e (mg/mL) are the initial concentration and equilibrium concentration of PSS, respectively, while m (mg/mL) is adsorbent dosage per volume. The experimental adsorption studies were conducted three times.

30 min, the mixed suspensions of alumina particles and PSS were shaken by hand, then the supernatants were separated using ultra-centrifugation at 18000 rpm for only 3 min with a centrifuge (EBA 21, HETTICH, Germany). On the one hand, when the adsorption time was longer than 30 min, the mixed suspensions were shaken for different time with a shaker (Cole Parmer 51704, USA). After the shaking, the Falcon tubes containing suspensions with PSS were taken and were centrifuged at 6000 rpm for 20 min with a centrifuge (DSC-200A-1,

Zeta potential measurements

Electrophoretic mobility measurement was used to evaluate the change in L-Al$_2$O$_3$ and S-Al$_2$O$_3$ surface electrokinetic charge before and after adsorption of PSS. The electrophoretic mobility was measured using a Zetasizer Nano ZS (Malvern) at a temperature of 25 °C, pH 4.0, and with 10 mM NaCl as a background electrolyte. The zeta potentials were calculated by measuring the electrophoretic mobility using Smoluchowski's equation [36] because the Debye length ~ 10 nm is smaller than the particle size.
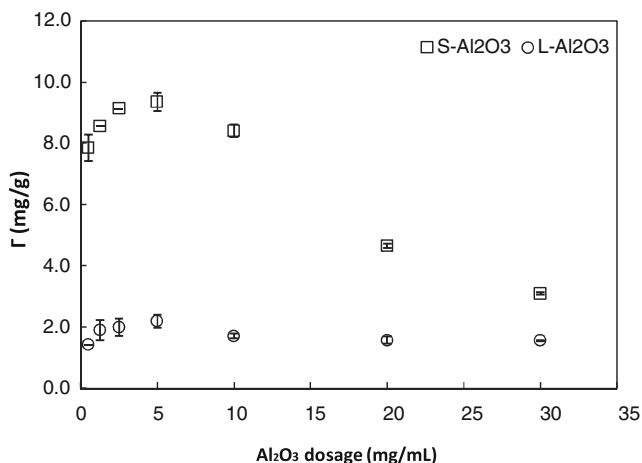

Fig. 2 Effect of adsorption time on PSS adsorption onto L-Al$_2$O$_3$ and S-Al$_2$O$_3$ (C_i (PSS) = 100 mg/L, pH 4, mass ratio of PSS to α-Al$_2$O$_3$ 20 mg/g, and 10 mM NaCl). Error bars show standard deviations of three replicates

Fig. 3 Effect of adsorbent dosage on PSS adsorption onto L-Al$_2$O$_3$ and S-Al$_2$O$_3$ (C_i (PSS) = 100 mg/L, adsorption time 120 min, pH 4, and 10 mM NaCl). Error bars show standard deviations of three replicates

$$\zeta = \frac{u_e \eta}{\varepsilon_{rs} \varepsilon_0} \qquad (2)$$

where ζ is the zeta potential (mV), u_e is the electrophoretic mobility (μm cm/sV), η is the dynamic viscosity of the liquid (mPa s), ε_{rs} is the relative permittivity constant of the electrolyte solution, and ε_0 is the electric permittivity of vacuum (8.854 × 10^{-12} F m^{-1}).

FT-IR spectroscopy

To determine the change of surface functional groups of L-Al$_2$O$_3$ and S-Al$_2$O$_3$ and to suggest the adsorption mechanism of PSS onto L-Al$_2$O$_3$ and S-Al$_2$O$_3$, FT-IR spectroscopy was performed with an Affinity-1S spectrometer (Shimadzu, Japan). The FT-IR spectra of L-Al$_2$O$_3$ and S-Al$_2$O$_3$ before and after PSS adsorption at the maximum level and PSS powder were obtained under at the same conditions including
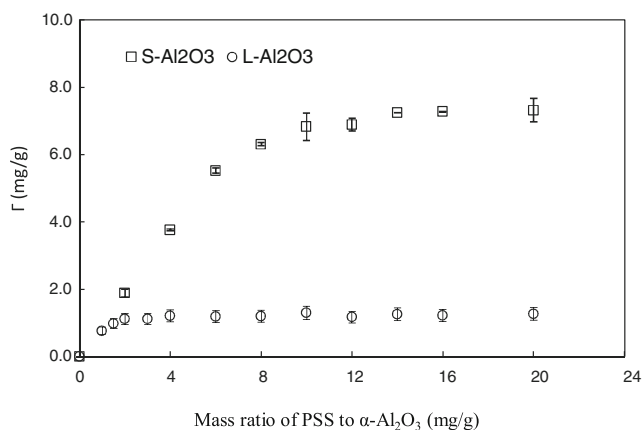

Fig. 4 Adsorption capacity of PSS onto L-Al$_2$O$_3$ and S-Al$_2$O$_3$ as a function of the mass ratio of PSS to α-Al$_2$O$_3$ at pH 4 in 10 mM NaCl concentrations. Error bars show standard deviations of three replicates

temperature 25 °C, atmospheric pressure, and resolution of 4 cm^{-1}.

Results and discussion

Effective conditions inducing adsorption of PSS onto L-Al$_2$O$_3$ and S-Al$_2$O$_3$

Effect of adsorption time

Adsorption time is important to ensure equilibrium of adsorption system. The effect of adsorption time on the PSS adsorption onto L-Al$_2$O$_3$ and S-Al$_2$O$_3$ is presented in Fig. 2 in which adsorption amount Γ is plotted as a function of adsorption time from 0 to 210 min. Adsorption of PSS onto L-Al$_2$O$_3$ and S-Al$_2$O$_3$ increased with increasing adsorption time. The plateau for S-Al$_2$O$_3$ was reached after 60 min while the plateau for L-Al$_2$O$_3$ was reached after 120 min. It suggests that adsorption of PSS onto S-Al$_2$O$_3$ reaches to the equilibrium faster than that onto L-Al$_2$O$_3$. Figure 2 also indicates that all standard deviations of three replicates are small, demonstrating the high repeatability of experiments. Adsorption here takes faster than PSS adsorbed on very large α-Al$_2$O$_3$ beads in which variable-charged adsorbent took place [19]. For PSS adsorption on hematite, charge regulation occurred with proton concomitant so that equilibrium time was more than 18 h [28]. In the present case, we did not obtain the proton co-adsorption upon PSS adsorption onto both L-Al$_2$O$_3$ and S-Al$_2$O$_3$; therefore, adsorption time was only 120 min. Thus, 120 min was selected for further adsorption studies.

Effect of adsorbent dosage and mass ratio of polymer to adsorbent

The adsorbent dosage affects the total surface area of adsorbent and number of binding sites [37] that affect adsorption amount significantly. The amount of both L-Al$_2$O$_3$ and S-Al$_2$O$_3$ was studied in the range 0.5–30 mg/mL.

Figure 3 shows that PSS adsorption increased with increasing Al$_2$O$_3$ dosage from 0.5 to 5.0 mg/mL for L-Al$_2$O$_3$ and S-Al$_2$O$_3$. An increase of adsorbent dosage increases the net surface area. As the results, more adsorption of PSS molecules can occur on the Al$_2$O$_3$ surface. Nevertheless, once Al$_2$O$_3$ dosage is higher than 5 mg/mL, the adsorbed amounts decrease from the maximum ~9 mg/g because of the aggregation of colloidal particles in the presence of polyelectrolytes [5, 28, 38]. It implies that the effect of adsorbent dosage for the case of S-Al$_2$O$_3$ is much higher than that for L-Al$_2$O$_3$. From Fig. 3, the adsorbent dosage of 5 mg/mL equals to the stoichiometric dosage of polymer 20 mg/g is suitable for PSS adsorption onto both L-Al$_2$O$_3$ and S-Al$_2$O$_3$.
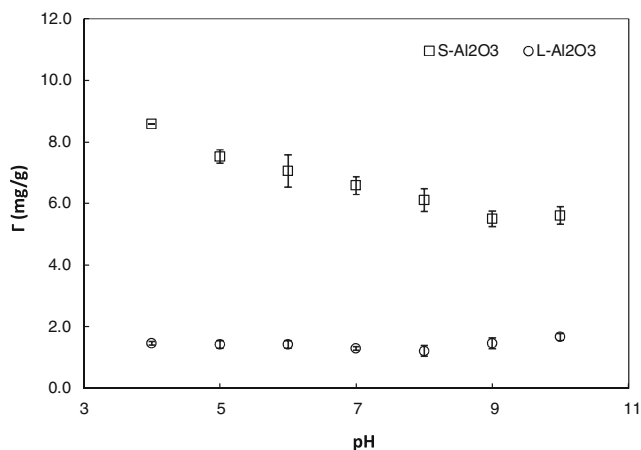
Fig. 5 Effect of pH on PSS adsorption onto L-Al$_2$O$_3$ and S-Al$_2$O$_3$ (C_i (PSS) = 100 mg/L, adsorption time 120 min, mass ratio of PSS to α-Al$_2$O$_3$ 20 mg/g, 10 mM NaCl). Error bars show standard deviations of three replicates

In order to evaluate the effect of PSS dosage, the adsorption capacity is plotted against the mass ratio of PSS to alumina while the amount of 5 mg/mL for L-Al$_2$O$_3$ and S-Al$_2$O$_3$ is fixed (Fig. 4). As can be seen from Fig. 4, the adsorption capacity of PSS onto L-Al$_2$O$_3$ and S-Al$_2$O$_3$ increased with increasing the mass ratio. The adsorption quickly reached the plateau at the mass ratio of 4 mg/g for L-Al$_2$O$_3$ while the PSS adsorption onto S-Al$_2$O$_3$ reached saturation at the mass ratio of 14 mg/g, since the specific surface area of S-Al$_2$O$_3$ is greater than that of L-Al$_2$O$_3$ 6.5 times. This is about 2.6 times higher than the differences in the mass ratio of PSS to alumina. Furthermore, the pore sizes of L-Al$_2$O$_3$ and S- Al$_2$O$_3$ which were determined by using the Barrett–Joyner–Halenda (BJH) model [39] to the N$_2$ desorption branch of isotherm were found to be
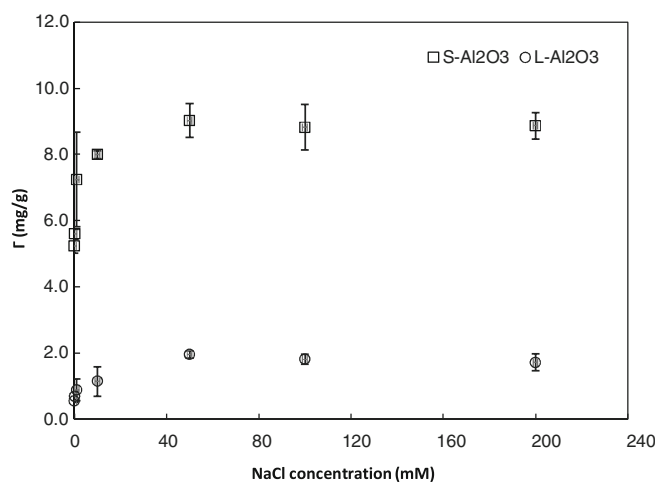
16.5 nm and 24.7 nm (data not shown). These pore sizes are higher than the hydrodynamic radius (Rh) of PSS [38]. It suggests that all the available PSS molecules were adsorbed on the surface of both L-Al$_2$O$_3$ and S-Al$_2$O$_3$ at a certain dosage, then adsorption of PSS could occur into pores of L-Al$_2$O$_3$ and S-Al$_2$O$_3$.

Effect of pH

Solution pH is one of the most important factors for polyelectrolyte adsorption because pH can influence to charging behavior of both adsorbent and adsorbate, since PSS is a strong polyanion that pH only affects to the surface charge of α-Al$_2$O$_3$ [40].

Figure 5 indicates the effect of pH on PSS adsorption onto L-Al$_2$O$_3$ and S-Al$_2$O$_3$. Open squares in Fig. 5 show that PSS adsorption onto S-Al$_2$O$_3$ decreases with decreasing pH from 4 to 9. With the increasing pH, the surface of S-Al$_2$O$_3$ has less positive charge that can prevent adsorption of polyanion PSS. On the other hand, the effect of pH on the PSS adsorption is not clear for L-Al$_2$O$_3$ (open circles) from pH 4 to pH 9. It should be noted that the mass ratio of PSS to L-Al$_2$O$_3$ and S-Al$_2$O$_3$ is kept as 20 mg/g corresponding to overdosing so that the adsorbent dosage here is not effective. As a result, surface charge of alumina as the function of pH affects to adsorption. These results could be explained by the low charge density of α-Al$_2$O$_3$ with a small specific surface area and insufficient electrostatic interaction at low PSS concentration [17, 19]. At pH > 9, when surface charge of α-Al$_2$O$_3$ is negative [41], the PSS adsorption onto L-Al$_2$O$_3$ and S-Al$_2$O$_3$ has a similar trend due to the presence of lateral interaction between PSS molecules. In order to evaluate the effect of electrostatic interaction and investigate effect of ionic strength, pH 4 was chosen and fixed for further study.
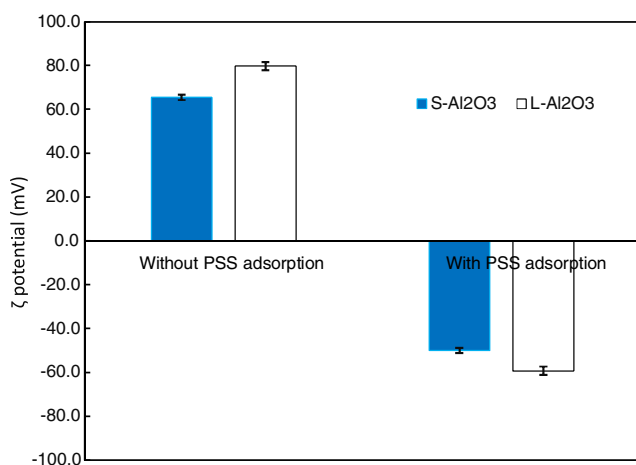
Fig. 6 Effect of NaCl concentration on PSS adsorption L-Al$_2$O$_3$ and S-Al$_2$O$_3$ (C_i (PSS) = 100 mg/L, adsorption time 120 min, mass ratio of PSS to α-Al$_2$O$_3$ 20 mg/g, pH 4). Error bars show standard deviations of three replicates

Fig. 7 The ζ potentials of L-Al_2O_3 and S-Al_2O_3 without and with PSS adsorption at pH 4 in 1 mM NaCl background electrolyte

Effect of ionic strength

Effect of ionic strength can be considered as the presence of salt with different concentrations in an adsorption system. Salt concentration affects PSS adsorption onto L-Al_2O_3 and S-Al_2O_3 because adsorption of PSS can be influenced by both electrostatic and non-electrostatic interactions [2, 19]. The experimental PSS adsorption onto L-Al_2O_3 and S-Al_2O_3 was carried out in NaCl concentrations from 0 to 200 mM at pH 4 (Fig. 6).

Figure 6 indicates that the adsorption amount of PSS on L-Al_2O_3 and S-Al_2O_3 increased with increasing NaCl concentration from 0 to 50 mM, suggesting that both electrostatic and non-electrostatic attraction can promote PSS adsorption onto L-Al_2O_3 and S-Al_2O_3. The

electrostatic attraction is screened with an increase of ionic strength while the different shapes of PSS [38] and more loops and tails of PSS can form on the surface of α-Al_2O_3 and the lateral repulsion between PSS molecules also decrease [19]. Nevertheless, when increasing salt higher than 50 mM, the adsorption capacity of PSS onto L-Al_2O_3 and S-Al_2O_3 seems to be constant.

Adsorption mechanisms of PSS onto L-Al_2O_3 and S-Al_2O_3

Adsorption mechanisms of PSS onto L-Al_2O_3 and S-Al_2O_3 are discussed in detail on the basis of surface charge change by ζ potential measurements and the change of functional groups by FT-IR.

Zeta (ζ) potential is powerful tool to evaluate the charging behavior of many materials [42, 43]. Among many techniques applied to measure ζ, electrophoretic mobility is the most common one. The ζ potentials of L-Al_2O_3 and S-Al_2O_3 particles without and with PSS adsorption at pH 4 and in 10 mM NaCl background electrolyte are shown in Fig. 7. The ζ potentials of L-Al_2O_3 and S-Al_2O_3 are about 79.70 and 65.45 mV, respectively. It implies that the surface charge of both L-Al_2O_3 and S-Al_2O_3 is highly positive and the ζ potentials of large particles are higher than that of the small ones. These results are in good agreement with the literatures [44, 45]. Nevertheless, the ζ potentials of L-Al_2O_3 and S-Al_2O_3 after PSS adsorption decrease dramatically because of the presence of strong polyanion. Due to numerous anionic sulfonate groups in the PSS molecules, surface charge is constant at the saturated adsorption level. Therefore, the charge of both L-Al_2O_3 and S-Al_2O_3 covered with PSS is highly negative.

Fig. 8 The ζ potentials of L-Al_2O_3 and S-Al_2O_3 against the mass ratio of PSS to α-Al_2O_3 at pH 4 in 10 mM NaCl background electrolyte
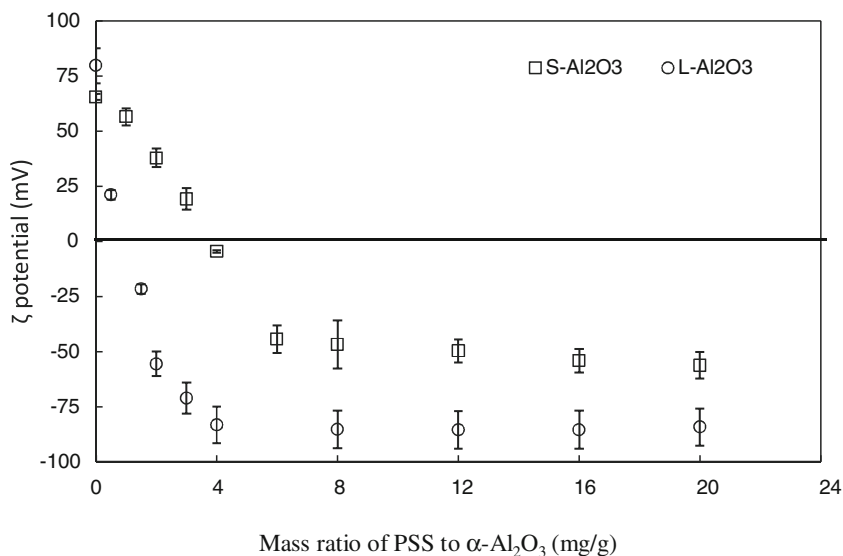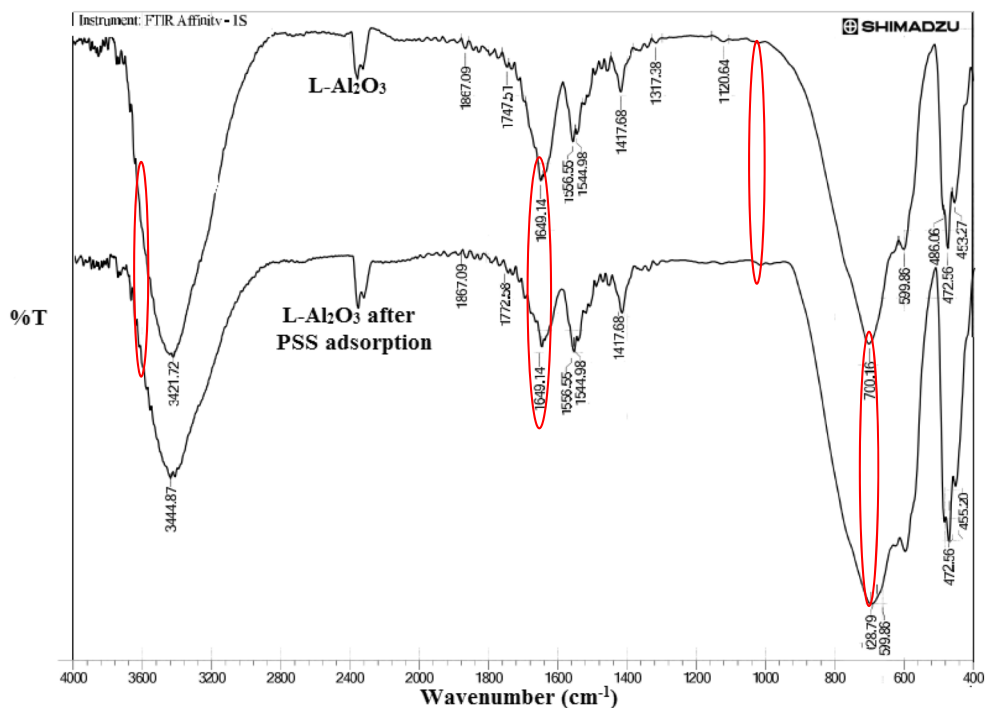
Fig. 9 FT-IR spectrum of L-Al_2O_3 particles before and after PSS adsorption in the wave number range of 400–4000 cm^{-1}


The results are in good agreement with the literature [46]. The ζ potential results suggest that the electrostatic interactions are dominant and the weak interactions are negligible. If the non-electrostatic interactions are dominant, the change in zeta potential must be small. Nevertheless, in this case, the zeta potential changes are significantly high.

In order to demonstrate the change of surface charge in more detail, the ζ potential is plotted against the mass ratio of PSS to L-Al_2O_3 and S-Al_2O_3 (Fig. 8). The ζ potential decreases with increasing the mass ratio of PSS to α-Al_2O_3,

then reaches a constant. The trends of ζ potential for L-Al_2O_3 and S-Al_2O_3 with increasing the mass ratio of PSS can be explained by the adsorption of negatively charged PSS onto surface of L-Al_2O_3 and S-Al_2O_3 inducing the negative charge. The plateau of ζ potential corresponds to the almost saturation of the adsorption of PSS onto L-Al_2O_3 and S-Al_2O_3 at the mass ratio of PSS to α-Al_2O_3 of 4 and 10 mg/g, respectively. Figure 9 also shows that the isoelectric points are found at the mass ratio of PSS to L-Al_2O_3 and S-Al_2O_3 as 1 mg/g and 4 mg/g, respectively. We obtain the good agreement of the

Fig. 10 FT-IR spectrum of S-Al_2O_3 particles before and after PSS adsorption in the wave number range of 400–4000 cm^{-1}
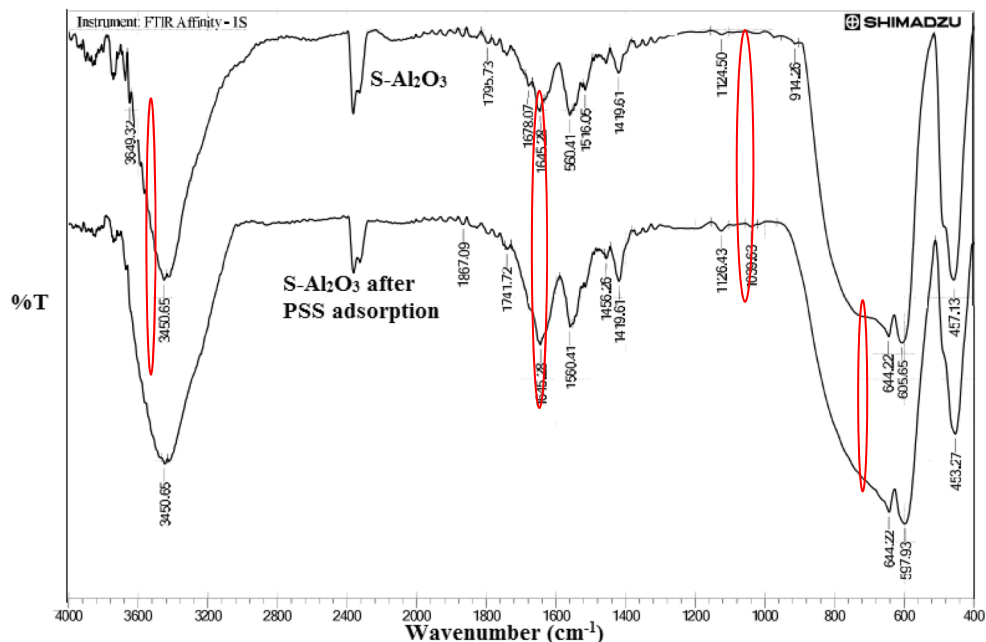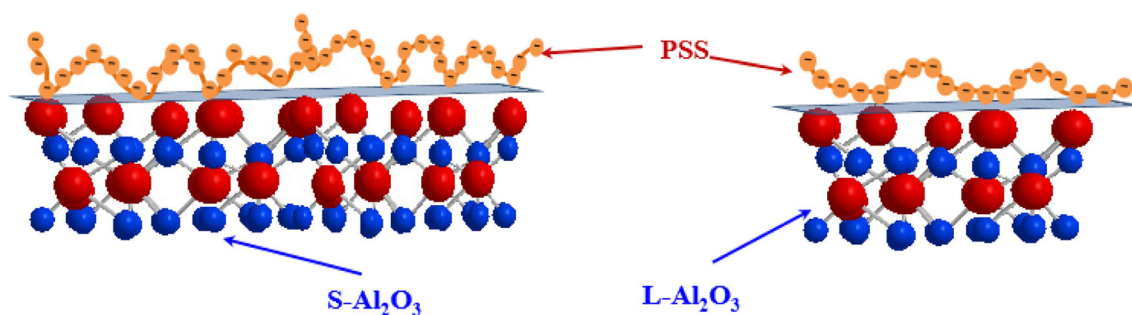
Fig. 11 Cartoon representation of structures of the adsorbed PSS onto L-Al$_2$O$_3$ and S-Al$_2$O$_3$

saturation adsorption between adsorbed amount and ζ potential measurements against the mass ratio of PSS to α-Al$_2$O$_3$.

Adsorption mechanism of PSS onto L-Al$_2$O$_3$ and S-Al$_2$O$_3$ is also discussed by the FT-IR spectrum of L-Al$_2$O$_3$ and S-Al$_2$O$_3$ before and after PSS adsorption (Figs. 9 and 10). The asymmetric and symmetric bands of PSS at 1185 and 1039 cm^{-1} [47] disappeared after adsorption onto L-Al$_2$O$_3$, while a small symmetric band of 1039 cm^{-1} appeared on the surface of S-Al$_2$O$_3$ after PSS adsorption. In addition, Figs. 9 and 10 show that after PSS adsorption, the intensity of peak characterized for at 1649 cm^{-1} for L-Al$_2$O$_3$ decreased while the peak intensity at 1645 cm^{-1} of S-Al$_2$O$_3$ increased. It suggests that PSS adsorption onto S-Al$_2$O$_3$ is stronger than that onto L-Al$_2$O$_3$. Furthermore, the stretching of C-S groups in PSS molecules at 676 cm^{-1} and the peaks at 3638 cm^{-1} assigned for O-H stretching of water molecule [48] could not be observed in FT-IR spectrum of both L-Al$_2$O$_3$ and S-Al$_2$O$_3$ after PSS adsorption. The results demonstrate that the adsorption of PSS molecules on L-Al$_2$O$_3$ and S-Al$_2$O$_3$ surface at the concentration is higher than that of the saturation through electrostatic attraction and hydrophobic interaction.

The results of the ζ potential after adsorption and ζ potential against the mass ratio of PSS to α-Al$_2$O$_3$ agreed well FT-IR spectrum, indicating that the PSS adsorbed onto L-Al$_2$O$_3$ and S-Al$_2$O$_3$ through the electrostatic attraction between negative PSS molecules with anionic sulfonate groups and the positively charged Al$_2$O$_3$ surface. This is similar to PSS adsorption on layered double hydroxide Zn$_2$Al(OH)$_6$Cl.nH$_2$O, where the interaction is by hydrogen bonding via the path S=O… H-O-Me [47]. In addition, the adsorbed amount as a function of the mass ratio of PSS to α-Al$_2$O$_3$, we confirm that PSS molecules may be responsible to form many bridges between the Al$_2$O$_3$ particles through the strong electrostatic and weak non-electrostatic interactions. Although the adsorption characteristics and mechanisms of PSS onto S-Al$_2$O$_3$ are similar to L-Al$_2$O$_3$, the plateau of PSS adsorption onto L-Al$_2$O$_3$ is much smaller than that onto S-Al$_2$O$_3$. The adsorption of PSS onto L-Al$_2$O$_3$ is also lower than that onto S-Al$_2$O$_3$ because the conformation of PSS onto L-Al$_2$O$_3$ with a smaller specific surface area is

more flat than for S-Al$_2$O$_3$. The more flat conformation for PSS is, the more adsorbed PSS is. In Fig. 11, a schematic representation shows the different structures of adsorbed PSS onto L-Al$_2$O$_3$ and S-Al$_2$O$_3$ at the same ionic strength. As can be seen in Fig. 11, based on the less flat conformation, adsorbed layer PSS appears with more loops onto S-Al$_2$O$_3$ with a large specific area than onto L-Al$_2$O$_3$. Our results indicate that particle size of α-Al$_2$O$_3$ is very important role in PSS adsorption system.

Conclusions

Adsorption of anionic polyelectrolyte, poly(styrene sulfonate), PSS, onto large L-Al$_2$O$_3$ and small S-Al$_2$O$_3$ particles was investigated in the present study. Optimum adsorption conditions of PSS onto both L-Al$_2$O$_3$ and S-Al$_2$O$_3$ were found to be adsorption time 120 min, the mass ratio of PSS to α-Al$_2$O$_3$ 20 mg/g, and ionic strength 50 mM NaCl. The pH of solution influenced to PSS adsorption onto S-Al$_2$O$_3$ was much higher than PSS adsorption onto L-Al$_2$O$_3$. The surface charge change by measuring the ζ potential as a function of the mass ratio of PSS to α-Al$_2$O$_3$ demonstrates that electrostatic interactions are the most important for PSS adsorption onto L-Al$_2$O$_3$ and S-Al$_2$O$_3$. The surface modification of L-Al$_2$O$_3$ and S-Al$_2$O$_3$ after PSS adsorption by Fourier-transform infrared spectroscopy (FT-IR) agreed with the change in surface charge of L-Al$_2$O$_3$ and S-Al$_2$O$_3$ and adsorbed amount as a function of the mass ratio of PSS to α-Al$_2$O$_3$, indicating that adsorption of PSS onto both L-Al$_2$O$_3$ and S-Al$_2$O$_3$ was induced by electrostatic and non-electrostatic interactions. In addition, adsorption of PSS is strongly influenced by particle size of α-Al$_2$O$_3$.

Compliance with ethical standards

Conflict of interest　The authors declare that they have no conflict of interest.

References

1. Bolto B, Gregory J (2007) Organic polyelectrolytes in water treatment. Water Res 41(11):2301–2324. https://doi.org/10.1016/j.watres.2007.03.012

2. Blokhus AM, Djurhuus K (2006) Adsorption of poly(styrene sulfonate) of different molecular weights on α-alumina: effect of added sodium dodecyl sulfate. J Colloid Interface Sci 296(1):64–70. https://doi.org/10.1016/j.jcis.2005.08.038

3. De Laat AWM (1995) Adsorption of water-soluble polymers onto barium titanate and its effect on colloidal stability, Doctoral Dissertation, Wagenigen University

4. Mishael YG, Dubin PL (2005) Uptake of organic pollutants by silica−polycation-immobilized micelles for groundwater remediation. Environ Sci Technol 39(21):8475–8480. https://doi.org/10.1021/es050763s

5. Pham TD, Bui TT, Nguyen VT, Bui TKV, Tran TT, Phan QC, Pham TD, Hoang TH (2018) Adsorption of polyelectrolyte onto nanosilica synthesized from rice husk: characteristics, mechanisms, and application for antibiotic removal. Polymers 10(2):220

6. Popuri SR, Vijaya Y, Boddu VM, Abburi K (2009) Adsorptive removal of copper and nickel ions from water using chitosan coated PVC beads. Bioresour Technol 100:194

7. Radian A, Mishael YG (2008) Characterizing and designing polycation−clay nanocomposites as a basis for imazapyr controlled release formulations. Environ Sci Technol 42(5):1511–1516. https://doi.org/10.1021/es7023753

8. Adachi Y, Kobayashi A, Kobayashi M (2012) Structure of colloidal flocs in relation to the dynamic properties of unstable suspension. Int J Polym Sci 2012:14. https://doi.org/10.1155/2012/574878

9. Adamczyk Z, Zembala M, Michna A (2006) Polyelectrolyte adsorption layers studied by streaming potential and particle deposition. J Colloid Interface Sci 303(2):353–364. https://doi.org/10.1016/j.jcis.2006.07.083

10. Hoogeveen NG, Stuart MAC, Fleer GJ (1996) Polyelectrolyte adsorption on oxides: I. Kinetics and adsorbed amounts. J Colloid Interface Sci 182(1):133–145. https://doi.org/10.1006/jcis.1996.0444

11. Porus M, Maroni P, Borkovec M (2012) Structure of adsorbed polyelectrolyte monolayers investigated by combining optical reflectometry and piezoelectric techniques. Langmuir 28(13):5642–5651. https://doi.org/10.1021/la204855j

12. Ramachandran R, Somasundaran P (1988) Polyelectrolyte interactions at the hematite/water interface. Part 1. Colloids Surfaces 32:307–317. https://doi.org/10.1016/0166-6622(88)80025-8

13. Shengcong L, Hanning X, Yuping L (2005) Adsorption of polyelectrolyte on the surface of ZnO nanoparticles and the stability of colloidal dispersions. Chin Sci Bull 50(15):1570–1575. https://doi.org/10.1360/982004-575

14. Wolterink JK (2003) Polyelectrolyte behavior in solution and at interfaces. Doctoral dissertation. Wagenigen University, Netherlands

15. Neivandt DJ, Gee ML, Tripp CP, Hair ML (1997) Coadsorption of poly(styrenesulfonate) and cetyltrimethylammonium bromide on silica investigated by attenuated Total reflection techniques. Langmuir 13(9):2519–2526. https://doi.org/10.1021/la962047x

16. Hase M, Scheffelmaier R, Hayden S, Rivera D (2010) Quantitative in situ attenuated total internal reflection Fourier transform infrared study of the isotherms of poly(sodium 4-styrene sulfonate) adsorption to a TiO2 surface over a range of cetylpyridinium bromide monohydrate concentration. Langmuir 26(8):5534–5543. https://doi.org/10.1021/la903787t

17. Sontum PC, Nöevestad A, Fahlvik AK, Gundersen HG (1996) Adsorption of poly(sodium(4)styrenesulfonate) on colloidal iron oxide particles. Int J Pharm 128(1–2):269–275. https://doi.org/10.1016/0378-5173(95)04330-6

18. Esumi K, Masuda A, Otsuka H (1993) Adsorption of poly(styrenesulfonate) and ionic surfactant from their binary mixtures of alumina. Langmuir 9(1):284–287. https://doi.org/10.1021/la00025a054

19. Pham TD, Kobayashi M, Adachi Y (2014) Adsorption of polyanion onto large alpha alumina beads with variably charged surface. Adv Phys Chem 2014:9. https://doi.org/10.1155/2014/460942

20. Dasgupta J, Singh A, Kumar S, Sikder J, Chakraborty S, Curcio S, Arafat HA (2016) Poly (sodium-4-styrenesulfonate) assisted ultrafiltration for methylene blue dye removal from simulated wastewater: optimization using response surface methodology. J Environ Chem Eng 4(2):2008–2022. https://doi.org/10.1016/j.jece.2016.03.033

21. Dejeu J, Buisson L, Guth MC, Roidor C, Membrey F, Charraut D, Foissy A (2006) Early steps of the film growth mechanism in self-assembled multilayers of PAH and PSS on silica: polymer uptake, charge balance and AFM analysis. Colloids Surf A Physicochem Eng Asp 288(1–3):26–35. https://doi.org/10.1016/j.colsurfa.2006.03.050

22. Čakara D, Kobayashi M, Skarba M, Borkovec M (2009) Protonation of silica particles in the presence of a strong cationic polyelectrolyte. Colloids Surf A Physicochem Eng Asp 339(1–3):20–25. https://doi.org/10.1016/j.colsurfa.2009.01.011

23. Mishael YG, Dubin PL, de Vries R, Kayitmazer AB (2007) Effect of pore size on adsorption of a polyelectrolyte to porous glass. Langmuir 23(5):2510–2516. https://doi.org/10.1021/la062314r

24. Vermöhlen K, Lewandowski H, Narres HD, Schwuger MJ (2000) Adsorption of polyelectrolytes onto oxides — the influence of ionic strength, molar mass, and Ca2+ ions. Colloids Surf A Physicochem Eng Asp 163(1):45–53. https://doi.org/10.1016/S0927-7757(99)00429-X

25. Dao TH, Tran TT, Nguyen VR, Pham TNM, Vu CM, Pham TD (2018) Removal of antibiotic from aqueous solution using synthesized TiO2 nanoparticles: characteristics and mechanisms. Environ Earth Sci 77(10):359. https://doi.org/10.1007/s12665-018-7550-z

26. Pham TD, Kobayashi M, Adachi Y (2015) Adsorption of anionic surfactant sodium dodecyl sulfate onto alpha alumina with small surface area. Colloid Polym Sci 293(1):217–227. https://doi.org/10.1007/s00396-014-3409-3

27. Pham TD, Kobayashi M, Adachi Y (2015) Adsorption characteristics of anionic azo dye onto large α-alumina beads. Colloid Polym Sci 293(7):1877–1886. https://doi.org/10.1007/s00396-015-3576-x

28. Wolterink JK, Koopal LK, Stuart MAC, Van Riemsdijk WH (2006) Surface charge regulation upon polyelectrolyte adsorption, hematite, polystyrene sulfonate, surface charge regulation: theoretical calculations and hematite-poly(styrene sulfonate) system. Colloids Surf A Physicochem Eng Asp 291(1–3):13–23. https://doi.org/10.1016/j.colsurfa.2006.04.053

29. De Laat AWM, van den Heuvel GLT (1995) Molecular weight fractionation in the adsorption of polyacrylic acid salts onto BaTiO3. Colloids Surf A Physicochem Eng Asp 98(1–2):53–59. https://doi.org/10.1016/0927-7757(95)03096-V

30. Jiang S, Xu H, Du N, Song S, Hou W (2018) Adsorption of benzyldimethyldodecylammonium bromide on silica nanoparticles in water. Colloid Polym Sci 296(2):341–353. https://doi.org/10.1007/s00396-017-4256-9

31. Tsai WT, Lai CW, Hsien KJ (2003) Effect of particle size of activated clay on the adsorption of paraquat from aqueous solution. J

Colloid Interface Sci 263(1):29–34. https://doi.org/10.1016/S0021-9797(03)00213-3

32. Yang L, Dadwhal M, Shahrivari Z, Ostwal M, Liu PKT, Sahimi M, Tsotsis TT (2006) Adsorption of arsenic on layered double hydroxides: effect of the particle size. Ind Eng Chem Res 45(13):4742–4751. https://doi.org/10.1021/ie051457q

33. Pham TD, Nguyen HH, Nguyen NV, Vu TT, Pham TNM, Doan THY, Nguyen MH, Ngo TMV (2017) Adsorptive removal of copper by using surfactant modified laterite soil. J Chem 2017:10. https://doi.org/10.1155/2017/1986071

34. Petzold G, Schwarz S (2006) Dye removal from solutions and sludges by using polyelectrolytes and polyelectrolyte–surfactant complexes. Sep Purif Technol 51(3):318–324. https://doi.org/10.1016/j.seppur.2006.02.016

35. Pham TD, Kobayashi M, Adachi Y (2013) Interfacial characterization of α-alumina with small surface area by streaming potential and chromatography. Colloids Surf A Physicochem Eng Asp 436(0):148–157. https://doi.org/10.1016/j.colsurfa.2013.06.026

36. Delgado AV, González-Caballero F, Hunter RJ, Koopal LK, Lyklema J (2007) Measurement and interpretation of electrokinetic phenomena. J Colloid Interface Sci 309(2):194–224

37. Pham TD, Do TT, Ha VL, Doan THY, Nguyen TAH, Mai TD, Kobayashi M, Adachi Y (2017) Adsorptive removal of ammonium ion from aqueous solution using surfactant-modified alumina. Environ Chem 14(5):327–337. https://doi.org/10.1071/EN17102

38. Adamczyk Z, Zembala M, Warszyński P, Jachimska B (2004) Characterization of polyelectrolyte multilayers by the streaming potential method. Langmuir 20(24):10517–10525. https://doi.org/10.1021/la040064d

39. Barrett EP, Joyner LG, Halenda PP (1951) The determination of pore volume and area distributions in porous substances. I. Computations from nitrogen isotherms. J Am Chem Soc 73(1):373–380. https://doi.org/10.1021/ja01145a126

40. Guzman E, Ritacco H, Rubio JEF, Rubio RG, Ortega F (2009) Salt-induced changes in the growth of polyelectrolyte layers of poly(diallyl-dimethylammonium chloride) and poly(4-styrene sulfonate of sodium). Soft Matter 5(10):2130–2142. https://doi.org/10.1039/b901193e

41. Franks GV, Meagher L (2003) The isoelectric points of sapphire crystals and alpha-alumina powder. Colloids Surf A Physicochem Eng Asp 214(1–3):99–110

42. Kobayashi M (2008) Electrophoretic mobility of latex spheres in the presence of divalent ions: experiments and modeling. Colloid Polym Sci 286(8–9):935–940. https://doi.org/10.1007/s00396-008-1851-9

43. Yamaguchi A, Kobayashi M (2016) Quantitative evaluation of shift of slipping plane and counterion binding to lysozyme by electrophoresis method. Colloid Polym Sci 294(6):1019–1026. https://doi.org/10.1007/s00396-016-3852-4

44. Kosmulski M (2016) Isoelectric points and points of zero charge of metal (hydr)oxides: 50 years after Parks' review. Adv Colloid Interf Sci 238:1–61. https://doi.org/10.1016/j.cis.2016.10.005

45. Vorwerg L, Antonietti M, Tauer K (1999) Electrophoretic mobility of latex particles: effect of particle size and surface structure. Colloids Surf A Physicochem Eng Asp 150(1):129–135. https://doi.org/10.1016/S0927-7757(98)00805-X

46. Szilagyi I, Trefalt G, Tiraferri A, Maroni P, Borkovec M (2014) Polyelectrolyte adsorption, interparticle forces, and colloidal aggregation. Soft Matter 10(15):2479–2502. https://doi.org/10.1039/c3sm52132j

47. Moujahid EM, Inacio J, Besse J-P, Leroux F (2003) Adsorption of styrene sulfonate vs. polystyrene sulfonate on layered double hydroxides. Microporous Mesoporous Mater 57(1):37–46. https://doi.org/10.1016/S1387-1811(02)00505-X

48. Duman O, Tunç S, Çetinkaya A (2012) Electrokinetic and rheological properties of kaolinite in poly(diallyldimethylammonium chloride), poly(sodium 4-styrene sulfonate) and poly(vinyl alcohol) solutions. Colloids Surf A Physicochem Eng Asp 394:23–32. https://doi.org/10.1016/j.colsurfa.2011.11.018